Acta Cryst E CRYSTALLOGRAPHIC COMMUNICATIONS

ISSN 2056-9890

Single crystals of $SnTe_3O_8$ in the millimetre range grown by chemical vapor transport reactions

Michael Ketter and Matthias Weil*

Institute for Chemical Technologies and Analytics, Division of Structural Chemistry, TU Wien, Getreidemarkt 9/164-SC, A-1060 Vienna, Austria. *Correspondence e-mail: matthias.weil@tuwien.ac.at

Received 5 November 2021
Accepted 8 November 2021

Edited by W. T. A. Harrison, University of Aberdeen, Scotland

Keywords: crystal structure; oxidotellurates; isotypism; electron lone pair.

CCDC reference: 2120742

Supporting information: this article has supporting information at journals.iucr.org/e

Tin(IV) trioxidotellurate(IV), $SnTe_3O_8$, is a member of the isotypic $M^{IV}Te^{IV}{}_3O_8$ (M = Ti, Zr, Hf, Sn) series crystallizing with eight formula units per unit cell in space group $Ia\bar{3}$. In comparison with the previous crystal structure model of $SnTe_3O_8$ based on powder X-ray diffraction data [Meunier & Galy (1971). *Acta Cryst.* B**27**, 602–608], the current model based on single-crystal X-ray data is improved in terms of precision and accuracy. Nearly regular [SnO_6] octahedra (Sn site symmetry .$\bar{3}$.) are situated in the voids of an oxidotellurate(IV) framework built up by corner-sharing [TeO_4] bisphenoids (Te site symmetry 2..). A quantitative structural comparison revealed a very high degree of similarity for the structures with M = Ti, Zr, Sn in the $M^{IV}Te_3O_8$ series.

1. Chemical context

The crystal chemistry of oxidotellurates(IV) is dominated by the presence of the $5s^2$ electron lone pair that, in the majority of cases, is stereochemically active, thus enabling one-sided coordination spheres around the Te^{IV} atom (Christy *et al.*, 2016). This peculiar building block often results in compounds with non-centrosymmetric structures or structures with polar directions exhibiting interesting physical properties (Ra *et al.*, 2003; Kim *et al.*, 2014). In this context, the microwave dielectric properties of $M^{IV}Te_3O_8$ (M = Sn, Zr) ceramics were investigated some time ago (Subodh & Sebastian, 2008).

The crystal structure of the isotypic series $M^{IV}Te_3O_8$ was originally determined for M = Ti from a single crystal in space group $Ia\bar{3}$ using photographic Weissenberg X-ray data, whereas for M = Sn, Zr and Hf, the crystal structures were refined from powder X-ray data (Meunier & Galy, 1971). In subsequent studies, crystal-structure refinements on the basis of single-crystal X-ray data were reported for the mineral winstanleyite with composition $(Ti_{0.96}Fe_{0.04})Te_3O_8$ (Bindi & Cipriani, 2003), and for the synthetic compound $ZrTe_3O_8$ (Noguera *et al.*, 2003; Lu *et al.*, 2019). A powder X-ray study of the solid solution $Sn_{0.59}Ti_{0.41}Te_3O_8$ crystallizing in the $M^{IV}Te_3O_8$ structure type has also been reported (Ben Aribia *et al.*, 2008).

Single-crystal growth of oxidotellurates(IV) can be accomplished through various crystallization methods including, for example, experiments under hydrothermal conditions (Weil *et al.*, 2018), cooling from the melt (Stöger *et al.*, 2009), from salt melts as fluxing agents (Weil, 2019), or from chemical vapor transport reactions (Missen *et al.*, 2020). The latter method (Binnewies *et al.*, 2012) is particularly suitable for growing large crystals of high quality and was the

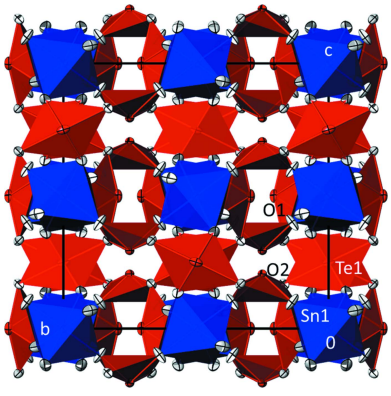

Table 1
Selected geometric parameters (Å, °).

Sn1—O1^{i}	2.0421 (11)	Te1—O2	2.1278 (3)
Te1—O1^{ii}	1.8800 (11)		
O1^{iii}—Te1—O1^{ii}	102.42 (8)	O2^{iv}—Te1—O2	157.05 (6)
O1^{iii}—Te1—O2	86.60 (6)	Te1—O2—Te1^{v}	117.94 (2)
O1^{ii}—Te1—O2	79.05 (4)		

Symmetry codes: (i) $-x+\frac{1}{2}, -y, z-\frac{1}{2}$; (ii) $-z+\frac{1}{2}, -x+\frac{1}{2}, -y+\frac{1}{2}$; (iii) $-z+\frac{1}{2}, x-\frac{1}{2}, y$; (iv) $x, -y, -z+\frac{1}{2}$; (v) z, x, y.

method of choice for crystal growth of $SnTe_3O_8$ for which a more precise and accurate structure refinement appeared to be desirable.

2. Structural commentary

The asymmetric unit of $SnTe_3O_8$ comprises one Sn^{IV} atom, one Te^{IV} atom, and two oxide anions, residing on sites 8*a* (site symmetry .$\bar{3}$.), 24*d* (2..), 48*e* (1) and 16*c* (.3.), respectively. The tin atom is in an almost regular octahedral coordination by oxygen, with six equal Sn1—O1 distances, all *trans* angles equal to 180°, and *cis* angles ranging from 86.09 (4) to 93.91 (4)°. The Te1 site is coordinated by four O atoms in pairs of shorter (O1) and longer distances (O2) (Table 1). The resulting [TeO_4] coordination polyhedron is a distorted bisphenoid. Considering the $5s^2$ electron lone pair at the Te^{IV} atom, the corresponding [ΨTeO_4] polyhedron has a shape intermediate between a square pyramid and a trigonal bipyramid with the non-bonding electron pair occupying an equatorial position (Fig. 1). The geometry index τ_5 of the [ΨTeO_4] polyhedron is 0.471 (τ_5 = 0 for an ideal square pyramid and τ_5 = 1 for an ideal trigonal bipyramid; Addison *et al.*, 1984). The position of the electron lone pair was calculated with the *LPLoc* software (Hamani *et al.*, 2020), with resulting fractional coordinates of x = 0.28655, y = 0, z = 1/4. The radius of the electron lone pair was calculated to be 1.07 Å with a distance of 0.90 Å from the Te1 position. The coordination numbers of the oxide anions are two and three: O1 coordinates to Sn1 and Te1 at the shorter of the two Te1—O distances whereas O2 coordinates to three Te1 atoms at the longer of the two Te1—O distances.

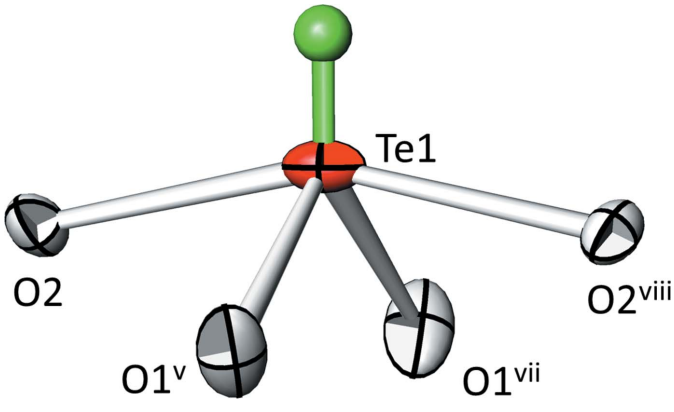

Figure 1
The coordination environment around Te1. Displacement ellipsoids are drawn at the 90% probability level; the electron lone pair is given as a green sphere of arbitrary radius. [Symmetry codes: (v) $-z+\frac{1}{2}, x-1/2, y$; (vii) $-z+\frac{1}{2}, -x+\frac{1}{2}, -y+\frac{1}{2}$; (viii) $x, -y, -z+\frac{1}{2}$.]

Table 2
Atom pairs and their absolute distances $|u|$ (Å) in the isotypic series MTe_3O_8 with $SnTe_3O_8$ as the reference structure, as well as degree of lattice distortion (S), arithmetic mean of the distances (d_{av}, Å) and measure of similarity (Δ).

	$TiTe_3O_8$ [a]	$(Ti_{0.96}Fe_{0.04})Te_3O_8$ [b]	$ZrTe_3O_8$ [c]	$ZrTe_3O_8$ [d]
M^{IV}1	0	0	0	0
Te1	0.0475	0.0360	0.0065	0.0059
O1	0.1061	0.0834	0.0713	0.0694
O2	0.1374	0.0968	0.0543	0.0446
S	0.0107	0.0102	0.0076	0.0092
d_{av}	0.0878	0.0668	0.0453	0.0436
Δ	0.011	0.008	0.006	0.006

Notes: (*a*) a = 10.956 (3) Å; Meunier & Galy (1971); (*b*) a = 10.965 (1) Å; Bindi & Cipriani (2003); (*c*) a = 11.308 (1) Å; Noguera *et al.* (2003); (*d*) a = 11.340 (4) Å; Lu *et al.* (2019).

In the crystal structure of $SnTe_3O_8$, the [SnO_6] octahedra are isolated from each other and arranged in rows running parallel to [100]. Each of the [TeO_4] bisphenoids shares corners (O2) with other [TeO_4] bisphenoids to form a three-dimensional oxidotellurate(IV) framework. The [SnO_6] octahedra are situated in the voids of this framework, thereby sharing each of the six corners with an individual [TeO_4] bisphenoid. The crystal structure of $SnTe_3O_8$ is depicted in Fig. 2.

The unit-cell parameter a from the previous powder X-ray study, 11.144 (3) Å, as well as interatomic distances of Sn1—O1 = 2.032 Å (6×), Te1—O1 = 1.850 Å (2×), Te1—O2 = 2.124 Å (2×), and angles O1—Te1—O1′ = 102.9°, and O2—

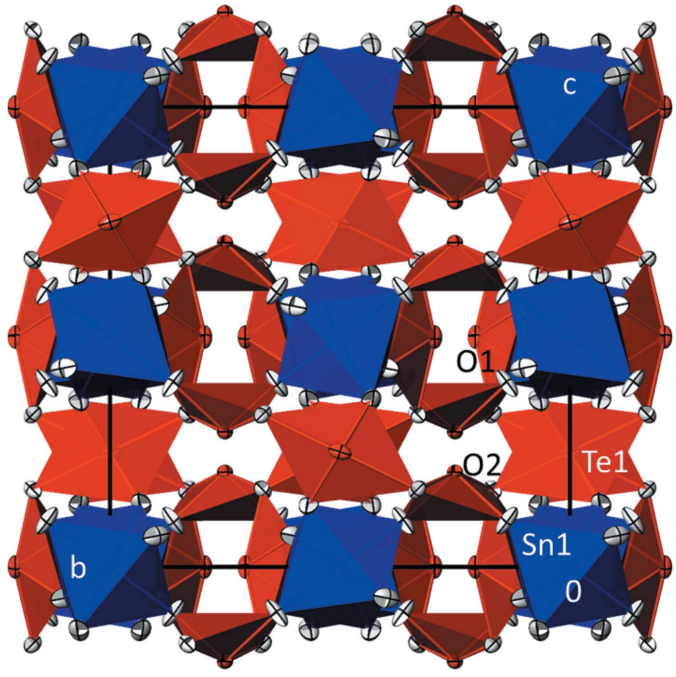

Figure 2
The crystal structure of $SnTe_3O_8$ in polyhedral representation, showing a projection along [$\bar{1}$00]. Displacement ellipsoids are as in Fig. 1; [TeO_4] polyhedra are red, [SnO_6] octahedra are blue.

Te1—O2′ = 156.8° (Meunier & Galy, 1971) agree with the present single-crystal study (Table 1), but with lower precision and accuracy. In comparison with the previous model based on powder X-ray data, the values of the bond-valence sums (Brown, 2002) using the parameters of Brese & O'Keeffe (1991) are much closer to the expected values of 4 for Sn and Te and 2 for O on basis of the current model [previous model: Sn1 4.28 valence units (v.u.), Te1 4.10 v.u., O1 2.09 v.u., O2 2.08 v.u.; current model: Sn1: 4.14 v.u., Te1 3.93 v.u., O1 1.99 v.u., O2 2.00 v.u.].

The relation of the isotypic crystal structures of $M^{IV}Te_3O_8$ compounds with that of the fluorite structure has been discussed previously for $TiTe_3O_8$ (Meunier & Galy, 1971; Wells, 1975). The unit-cell parameter a of cubic $TiTe_3O_8$ is ∼2a of cubic CaF_2, whereby the ordered distribution of the cationic sites leads to a doubling of the unit cell and also to a considerable distortion of the respective coordination environments. The original cubic coordination around the Ca^{II} cation in the fluorite structure is changed to an octahedral coordination of Sn^{IV} and a fourfold coordination of Te^{IV} in the superstructure of the $M^{IV}Te_3O_8$ compounds. Note that there are two additional O atoms at a distance of 3.2446 (19) Å around the M^{IV} site and two pairs of additional O atoms at a distance of 2.9076 (12) and 3.3957 (13) Å around the Te1 site in $SnTe_3O_8$, completing an eightfold coordination in each case. Correspondingly, each of the two O sites has a fourfold coordination in case the much longer distances are counted.

A quantitative structural comparison of the $M^{IV}Te_3O_8$ structures where single crystal data are available (M = Ti, Zr, Sn) was undertaken with the program *compstru* (de la Flor *et al.*, 2016) available at the Bilbao Crystallographic Server (Aroyo *et al.*, 2006). Table 2 lists the degree of lattice distortion (S), the maximum distance between the atomic positions of paired atoms ($|u|$), the arithmetic mean of all distances, and the measure of similarity (Δ) relative to $SnTe_3O_8$ as the reference structure. All these values show a very high similarity between the crystal structures in the isotypic $M^{IV}Te_3O_8$ series.

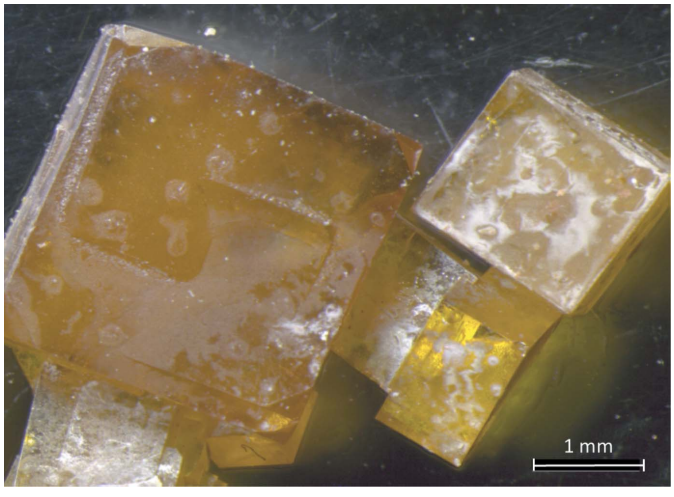

Figure 3
Photograph of Sn_3TeO_8 single crystals grown by chemical vapor transport reactions.

Table 3
Experimental details.

Crystal data	
Chemical formula	$SnTe_3O_8$
M_r	629.49
Crystal system, space group	Cubic, $Ia\overline{3}$
Temperature (K)	296
a (Å)	11.1574 (4)
V (Å^3)	1388.96 (15)
Z	8
Radiation type	Mo $K\alpha$
μ (mm^{-1})	16.04
Crystal size (mm)	0.06 × 0.06 × 0.01
Data collection	
Diffractometer	Bruker APEXII CCD
Absorption correction	Multi-scan (*SADABS*; Krause *et al.*, 2015)
T_{min}, T_{max}	0.452, 0.748
No. of measured, independent and observed [$I > 2\sigma(I)$] reflections	14087, 735, 697
R_{int}	0.048
(sin $\theta/\lambda)_{max}$ (Å^{-1})	0.907
Refinement	
$R[F^2 > 2\sigma(F^2)]$, $wR(F^2)$, S	0.014, 0.030, 1.07
No. of reflections	735
No. of parameters	21
$\Delta\rho_{max}$, $\Delta\rho_{min}$ (e Å^{-3})	1.27, −0.86

Computer programs: *APEX3* and *SAINT* (Bruker, 2018), *SHELXL* (Sheldrick, 2015), *ATOMS* (Dowty, 2006) and *publCIF* (Westrip, 2010).

3. Synthesis and crystallization

Reagent-grade chemicals were used without further purification. SnO_2 (71 mg, 0.47 mmol) and TeO_2 (225 mg, 1.40 mmol) were thoroughly mixed in the molar ratio 1:3 and placed in a silica tube to which 50 mg of $TeCl_4$ were added as the transport agent. The silica ampoule was then evacuated and torch-sealed, placed in a two-zone furnace using a temperature gradient 973 K (source) → 873 K (sink) for three days. Cubic, canary-yellow crystals had formed in the millimetre size range in the colder sink region as the only product (Fig. 3). Powder X-ray diffraction of the remaining material in the source region revealed $SnTe_3O_8$ as the main phase and SnO_2 as a side phase. For the single-crystal diffraction study, a fragment was broken from a larger crystal.

4. Refinement

Crystal data, data collection and structure refinement details are summarized in Table 3. Atomic coordinates and the labelling scheme were adapted from isotypic $TiTe_3O_8$ (Meunier & Galy, 1971).

Acknowledgements

The X-ray centre of the Vienna University of Technology is acknowledged for financial support and for providing access to the single-crystal and powder X-ray diffractometers.

References

Addison, A. W., Rao, T. N., Reedijk, J., van Rijn, J. & Verschoor, G. C. (1984). *J. Chem. Soc. Dalton Trans.* pp. 1349–1356.

Aroyo, M. I., Perez-Mato, J. M., Capillas, C., Kroumova, E., Ivantchev, S., Madariaga, G., Kirov, A. & Wondratschek, H. (2006). *Z. Kristallogr.* **221**, 15–27.

Ben Aribia, W., Loukil, M., Kabadou, A. & Ben Salah, A. (2008). *Powder Diffr.* **23**, 228–231.

Bindi, L. & Cipriani, C. (2003). *Can. Mineral.* **41**, 1469–1473.

Binnewies, M., Glaum, R., Schmidt, M. & Schmidt, P. (2012). *Chemical Vapor Transport Reactions*. Berlin, Boston: De Gruyter,.

Brese, N. E. & O'Keeffe, M. (1991). *Acta Cryst.* B**47**, 192–197.

Brown, I. D. (2002). *The Chemical Bond in Inorganic Chemistry: The Bond Valence Model.* Oxford University Press.

Bruker (2018). *APEX3* and *SAINT*. Bruker-AXS Inc. Madison, Wisconsin, USA.

Christy, A. G., Mills, S. J. & Kampf, A. R. (2016). *Miner. Mag.* **80**, 415–545.

Dowty, E. (2006). *ATOMS*. Shape Software, Kingsport, Tennessee, USA.

Flor, G. de la, Orobengoa, D., Tasci, E., Perez-Mato, J. M. & Aroyo, M. I. (2016). *J. Appl. Cryst.* **49**, 653–664.

Hamani, D., Masson, O. & Thomas, P. (2020). *J. Appl. Cryst.* **53**, 1243–1251.

Kim, Y. H., Lee, D. W. & Ok, K. M. (2014). *Inorg. Chem.* **53**, 5240–5245.

Krause, L., Herbst-Irmer, R., Sheldrick, G. M. & Stalke, D. (2015). *J. Appl. Cryst.* **48**, 3–10.

Lu, W., Gao, Z., Du, X., Tian, X., Wu, Q., Li, C., Sun, Y., Liu, Y. & Tao, X. (2019). *Inorg. Chem.* **58**, 7794–7802.

Meunier, G. & Galy, J. (1971). *Acta Cryst.* B**27**, 602–608.

Missen, O. P., Weil, M., Mills, S. J. & Libowitzky, E. (2020). *Acta Cryst.* B**76**, 1–6.

Noguera, O., Thomas, P., Masson, O. & Champarnaud-Mesjard, J. C. (2003). *Z. Kristallogr. New Cryst. Struct.* **218**, 293–294.

Ra, H.-S., Ok, K. M. & Halasyamani, P. S. (2003). *J. Am. Chem. Soc.* **125**, 7764–7765.

Sheldrick, G. M. (2015). *Acta Cryst.* C**71**, 3–8.

Stöger, B., Weil, M., Zobetz, E. & Giester, G. (2009). *Acta Cryst.* B**65**, 167–181.

Subodh, G. & Sebastian, M. T. (2008). *Jpn. J. Appl. Phys.* **47**, 7943–7946.

Weil, M. (2019). *Acta Cryst.* E**75**, 26–29.

Weil, M., Shirkhanlou, M., Füglein, E. & Libowitzky, E. (2018). *Crystals*, **8**, 51.

Wells, A. F. (1975). *Structural Inorganic Chemistry*, 4th ed, pp. 207–208. Oxford: Clarendon Press.

Westrip, S. P. (2010). *J. Appl. Cryst.* **43**, 920–925.

supporting information

Acta Cryst. (2021). E**77**, 1276-1279 [https://doi.org/10.1107/S2056989021011828]

Single crystals of $SnTe_3O_8$ in the millimetre range grown by chemical vapor transport reactions

Michael Ketter and Matthias Weil

Computing details

Data collection: *APEX3* (Bruker, 2018); cell refinement: *SAINT* (Bruker, 2018); data reduction: *SAINT* (Bruker, 2018); program(s) used to solve structure: coordinates from previous refinement; program(s) used to refine structure: *SHELXL* (Sheldrick, 2015); molecular graphics: *ATOMS* (Dowty, 2006); software used to prepare material for publication: *publCIF* (Westrip, 2010).

Tin(IV) trioxidotellurate(IV)

Crystal data

$SnTe_3O_8$
M_r = 629.49
Cubic, $Ia\bar{3}$
a = 11.1574 (4) Å
V = 1388.96 (15) Å^3
Z = 8
$F(000)$ = 2160
D_x = 6.021 Mg m^{-3}
Mo $K\alpha$ radiation, λ = 0.71073 Å
Cell parameters from 5266 reflections
θ = 3.7–38.9°
μ = 16.04 mm^{-1}
T = 296 K
Plate, light yellow
0.06 × 0.06 × 0.01 mm

Data collection

Bruker APEXII CCD diffractometer
ω– and φ–scans
Absorption correction: multi-scan (*SADABS*; Krause *et al.*, 2015)
T_{min} = 0.452, T_{max} = 0.748
14087 measured reflections
735 independent reflections
697 reflections with $I > 2\sigma(I)$
R_{int} = 0.048
θ_{max} = 40.2°, θ_{min} = 3.7°
h = −18→20
k = −20→20
l = −19→20

Refinement

Refinement on F^2
Least-squares matrix: full
$R[F^2 > 2\sigma(F^2)]$ = 0.014
$wR(F^2)$ = 0.030
S = 1.07
735 reflections
21 parameters
0 restraints
$w = 1/[\sigma^2(F_o^2) + (0.0127P)^2 + 1.9293P]$ where $P = (F_o^2 + 2F_c^2)/3$
$(\Delta/\sigma)_{max}$ = 0.001
$\Delta\rho_{max}$ = 1.27 e Å^{-3}
$\Delta\rho_{min}$ = −0.85 e Å^{-3}
Extinction correction: SHELXL-2017/1 (Sheldrick 2015), $Fc^*=kFc[1+0.001xFc^2\lambda^3/\sin(2\theta)]^{-1/4}$
Extinction coefficient: 0.00046 (3)

Special details

Geometry. All esds (except the esd in the dihedral angle between two l.s. planes) are estimated using the full covariance matrix. The cell esds are taken into account individually in the estimation of esds in distances, angles and torsion angles; correlations between esds in cell parameters are only used when they are defined by crystal symmetry. An approximate (isotropic) treatment of cell esds is used for estimating esds involving l.s. planes.

Fractional atomic coordinates and isotropic or equivalent isotropic displacement parameters (Å²)

	x	*y*	*z*	U_{iso}*/U_{eq}
Sn1	0.000000	0.000000	0.000000	0.00501 (4)
Te1	0.20584 (2)	0.000000	0.250000	0.00804 (4)
O1	0.43242 (10)	0.13738 (10)	0.39972 (11)	0.0129 (2)
O2	0.16789 (10)	0.16789 (10)	0.16789 (10)	0.0078 (3)

Atomic displacement parameters (Å²)

	U^{11}	U^{22}	U^{33}	U^{12}	U^{13}	U^{23}
Sn1	0.00501 (4)	0.00501 (4)	0.00501 (4)	−0.00031 (3)	−0.00031 (3)	−0.00031 (3)
Te1	0.00518 (5)	0.01273 (6)	0.00620 (5)	0.000	0.000	−0.00229 (4)
O1	0.0095 (4)	0.0117 (4)	0.0174 (5)	0.0019 (3)	0.0018 (4)	0.0094 (4)
O2	0.0078 (3)	0.0078 (3)	0.0078 (3)	0.0020 (3)	0.0020 (3)	0.0020 (3)

Geometric parameters (Å, º)

Sn1—O1^{i}	2.0421 (11)	Sn1—O1^{vi}	2.0421 (11)
Sn1—O1^{ii}	2.0421 (11)	Te1—O1^{v}	1.8800 (11)
Sn1—O1^{iii}	2.0421 (11)	Te1—O1^{vii}	1.8800 (11)
Sn1—O1^{iv}	2.0421 (11)	Te1—O2^{viii}	2.1278 (3)
Sn1—O1^{v}	2.0421 (11)	Te1—O2	2.1278 (3)
O1^{i}—Sn1—O1^{ii}	86.09 (4)	O1^{iv}—Sn1—O1^{vi}	93.91 (4)
O1^{i}—Sn1—O1^{iii}	93.91 (4)	O1^{v}—Sn1—O1^{vi}	86.09 (4)
O1^{ii}—Sn1—O1^{iii}	180.00 (9)	O1^{v}—Te1—O1^{vii}	102.42 (8)
O1^{i}—Sn1—O1^{iv}	86.09 (4)	O1^{v}—Te1—O2^{viii}	79.05 (4)
O1^{ii}—Sn1—O1^{iv}	93.91 (4)	O1^{vii}—Te1—O2^{viii}	86.60 (6)
O1^{iii}—Sn1—O1^{iv}	86.09 (4)	O1^{v}—Te1—O2	86.60 (6)
O1^{i}—Sn1—O1^{v}	93.91 (4)	O1^{vii}—Te1—O2	79.05 (4)
O1^{ii}—Sn1—O1^{v}	86.09 (4)	O2^{viii}—Te1—O2	157.05 (6)
O1^{iii}—Sn1—O1^{v}	93.91 (4)	Te1^{ix}—O1—Sn1^{x}	134.17 (6)
O1^{iv}—Sn1—O1^{v}	180.00 (9)	Te1—O2—Te1^{xi}	117.94 (2)
O1^{i}—Sn1—O1^{vi}	180.00 (9)	Te1—O2—Te1^{xii}	117.94 (2)
O1^{ii}—Sn1—O1^{vi}	93.91 (4)	Te1^{xi}—O2—Te1^{xii}	117.94 (2)
O1^{iii}—Sn1—O1^{vi}	86.09 (4)		

Symmetry codes: (i) *y*, −*z*+1/2, *x*−1/2; (ii) −*x*+1/2, −*y*, *z*−1/2; (iii) *x*−1/2, *y*, −*z*+1/2; (iv) *z*−1/2, −*x*+1/2, −*y*; (v) −*z*+1/2, *x*−1/2, *y*; (vi) −*y*, *z*−1/2, −*x*+1/2; (vii) −*z*+1/2, −*x*+1/2, −*y*+1/2; (viii) *x*, −*y*, −*z*+1/2; (ix) −*y*+1/2, −*z*+1/2, −*x*+1/2; (x) −*x*+1/2, −*y*, *z*+1/2; (xi) *z*, *x*, *y*; (xii) *y*, *z*, *x*.